J. Fluid Mech. (1985), vol. 159, pp. 303–321
Printed in Great Britain

Optimal discharge profiles for sudden contaminant releases in steady, uniform open-channel flow

By N. C. DAISH

Department of Applied Mathematics and Theoretical Physics, University of Cambridge, Silver Street, Cambridge CB3 9EW

(Received 24 August 1984 and in revised form 30 April 1985)

The effect of varying the initial concentration distribution is investigated for a sudden contaminant release in a uniform straight channel. Taking the optimal choice to be that which maximizes the variance of the contaminant cloud far downstream, it is found that, unless the topography is very unusual, the largest variance can be generated by splitting the contaminant into two parts, placing the larger part at the bank where the channel bed slopes most gently, and the remainder near to where the channel is deepest. This procedure significantly reduces peak concentrations far downstream when compared with making the entire release at any single point across the flow. Even at distances as large as six times the e-folding distance for cross-sectional mixing, the splitting of the discharge is shown to reduce the peak concentrations by a third.

1. Introduction

One of the ways in which shear-dispersion studies are useful to the problem of environmental pollution is in assessing the relative merit of different discharge conditions for a contaminant release. The goal of such studies should be to choose the source distribution that minimizes the effect of the release in one or more ways. For example, by a suitable choice of initial conditions, we might try to reduce the peak concentrations far downstream of the release as much as possible, or minimize the residence time of the contaminant in the flow.

For flows that are essentially steady in time, such as the mean flow in a river in its pretidal stages, the time of release is irrelevant, so that we should aim to optimize the spatial distribution. This presents a choice between two main types of contaminant discharge: sudden and continuous. The optimal siting of a continuous point release in a river has been investigated by Smith (1982*a*), who finds the best site to be near to the middle of such a channel; this keeps the contaminant plume formed away from the banks for as long as possible.

The other main type of release – the sudden discharge – results in a contaminant cloud, rather than a plume, which is swept downstream by the mean flow. Such a release would be appropriate to industrial users of a river with relatively small amounts of waste to dispose of. In this case, although an observer near to the point of release will experience a region of very high concentrations, particularly if the discharge is strongly localized, this will be a transitory region – quite a different situation from the steady-discharge case. We shall therefore focus attention on the behaviour of the cloud a long distance from the release, when it has had time to spread across the flow, and attempt to minimize the peak concentrations there, for example at a water intake some distance downstream of the user.

In the sections that follow, we shall arrive at a simple way of choosing the optimal source distribution for such a sudden contaminant release in a straight uniform channel with arbitrary depth profile. If we take 'optimal' to mean maximizing the variance of the concentration distribution far downstream, then we show that unless the channel has a very unusual topography the optimal choice for the distribution is to take just two point sources. We find that the first, more heavily weighted, source should be placed at the bank with the shallowest water adjacent to it, with the second sited near to the deepest part of the channel. This procedure significantly reduces the peak concentrations far downstream when compared with those produced by a single point discharge at one of the banks (as advocated by Smith 1981). The choice of split source is also more robust to variations in the depth profile than the single source: the best site for a single point discharge need not be at one of the banks if there is a favourable location in the channel interior, namely another region of shallow water (a possibility overlooked by Smith 1981), whereas the two-source procedure will be unaffected by such a feature unless it is exceptionally extensive.

2. Asymptotic form of the concentration: pipe flow

The general features of the evolution of a contaminant cloud far downstream of its release have been known for some time. The first to describe the most important characteristics that emerge after sufficient time has elapsed for the cloud to become fairly evenly distributed across the flow was Taylor (1953, 1954 *a*, *b*). He showed, in the case of laminar Poiseuille flow, that in a frame moving with the cross-sectionally averaged velocity $\overline{u}$ a contaminant cloud is eventually stationary, as characterized by its mass centroid, and the cross-sectional mean concentration $\bar{c}$ evolves as per a one-dimensional diffusion equation with an augmented diffusion coefficient D which can greatly exceed the molecular diffusivity κ (Taylor 1953). He found the same features in the evolution of a contaminant cloud in turbulent pipe flow, where now the longitudinal turbulent diffusivity κ_1 can be small compared with the coefficient D, which itself depends on the transverse turbulent diffusivity κ_2 (Taylor 1954*a*).

Aris (1956) also investigated dispersion in laminar pipe flow, calculating the asymptotic form of the spatial moments of the concentration $\{c^{(p)}\}_{p=0}^{\infty}$ rather than c itself. If (x, y, z) are Cartesian coordinates in a frame moving with the bulk velocity $\overline{u}$, with the x-axis occupying the centreline of the pipe, the pth moment $c^{(p)}(y, z, t)$ is defined by

$$c^{(p)}(y, z, t) = \int_{-\infty}^{\infty} x^p c(x, y, z, t)\, \mathrm{d}x, \tag{2.1}$$

where t is the time. The functions $\{c^{(p)}\}_{p=0}^{\infty}$ then describe the distribution of contaminant in a particular flow filament centred on $(y, z) =$ constant. In particular, $c^{(0)}$ gives the total mass of contaminant in the filament, $c^{(1)}/c^{(0)}$ gives the position of its centre of gravity and $c^{(2)}$ is related to the variance σ^2 through

$$\sigma^2 = \frac{c^{(2)}}{c^{(0)}} - \left\{\frac{c^{(1)}}{c^{(0)}}\right\}^2. \tag{2.2}$$

The cross-sectionally averaged moments $\{\overline{c^{(p)}}(t)\}_{p=0}^{\infty}$ give the corresponding information about the whole cloud.

Starting at $p = 0$, Aris found that $c^{(0)}$ tends to a constant far downstream, so that eventually there is equal mass in each flow filament. He confirmed that the centre of gravity of the cloud is asymptotically stationary, displaced a distance X from the origin of the moving frame, i.e.

$$\overline{c^{(1)}}/\overline{c^{(0)}} \sim X. \tag{2.3}$$

(Note that the asymptotic limit we are considering is, strictly speaking, that of $t \to \infty$; however, the asymptotic results that follow will all apply after a time of order b^2/ϵ, where b is a lengthscale for cross-sectional mixing and ϵ is a characteristic value of the diffusion coefficient across the flow.) The first moment itself becomes a function of y and z only,

$$c^{(1)}/c^{(0)} \sim X + g(y,z), \tag{2.4}$$

so that the centres of gravity of the filaments are distributed according to the function g. Aris observes that g also appears in Taylor's (1954*b*) expression for the asymptotic concentration:

$$c \sim \bar{c} - g(y,z)\frac{\partial \bar{c}}{\partial x} \tag{2.5}$$

(Taylor 1954*b*, equation (6)). Thus g gives the shape of the concentration profile within a particular cross-section as well, and is therefore referred to as the 'shape function'.

Finally, the second moment – and therefore the variance – grows with time as t; its asymptotic form is

$$\frac{c^{(2)}}{c^{(0)}} \sim 2\left(\kappa + \frac{\overline{u}^2 a^2}{48\kappa}\right)t + 2g^{(2)}(y,z) + \text{const}, \tag{2.6}$$

where the constant depends on the discharge conditions, but $g^{(2)}$ is independent of the initial concentration distribution. The time-dependence of $c^{(2)}$ is in agreement with the well-known property of the one-dimensional diffusion equation with a constant diffusion coefficient that the variance of the solution grows linearly with time (Fischer *et al.* 1979). The additional contribution to the growth rate is identical with the augmented diffusion coefficient, or dispersion coefficient D, found by Taylor (1953). Clearly, it can be much larger than κ; we shall henceforth neglect κ (or $\overline{\kappa}_1$ in the turbulent case) in favour of D. Aris shows that it is related to the shape function g through

$$D = \overline{(u-\overline{u})g}. \tag{2.7}$$

3. Asymptotic form of the concentration: open-channel flow

The results of §2 have been extended to the depth-averaged turbulent flow in an open channel, relevant to rivers and other 'natural streams', by Smith. Such a channel will be the underlying configuration in the rest of this paper, and is sketched in figure 1. It is straight and longitudinally uniform, with Cartesian coordinates (x,y,z) aligned along and across the flow as indicated. It has breadth B and maximum depth H, with a depth profile $h(y)$ which vanishes at each bank.

At $t = 0$ a sudden contaminant release is made at $x = 0$, with non-uniformities across the flow described by $q(y)$. If $\|\kappa_3\|$ is the depth-averaged vertical eddy diffusivity, the cloud from such a release will become vertically well-mixed after a distance of order $\overline{u}H^2/\|\kappa_3\|$ – typically about 40 water-depths – so we can treat it as vertically uniform for the purposes of our calculations. The initial condition for the concentration is therefore

$$c = q(y)\,\delta(x) \quad \text{at } t = 0. \tag{3.1}$$

Furthermore, because the channel is uniform, we can adopt the depth-averaged form of the dependent variables u and κ_2 throughout, so that these are now the depth-averaged mean turbulent velocity and transverse turbulent diffusivity respectively, and cross-sectionally averaged quantities become depth-weighted averages:

$$\bar{f} = \frac{1}{A}\int_0^B h(y) f(y)\,\mathrm{d}y, \tag{3.2}$$

where A is the cross-sectional area of the channel.

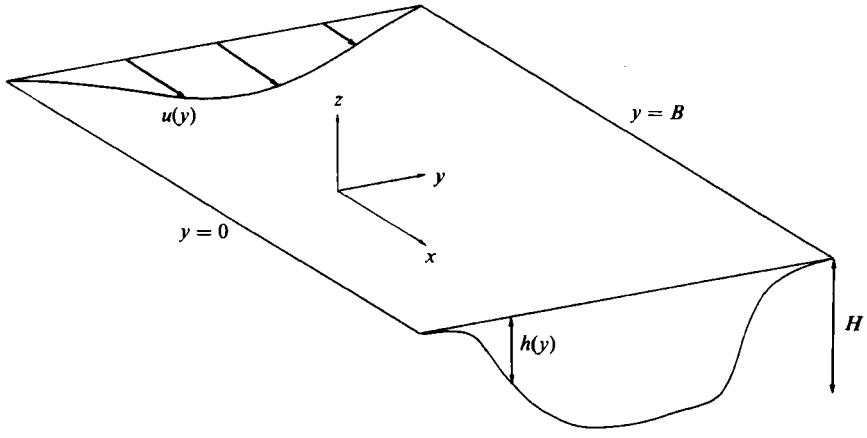

FIGURE 1. Sketch of configuration: uniform straight channel.

u and κ_2 are assumed to vary with y as powers of the local depth h: this guarantees that the velocity is greatest and the transverse mixing most vigorous in the deepest parts of the channel, in accordance with observation, as well as providing a convenient representation of these quantities. Throughout the rest of this paper we employ the specific choice of a velocity profile that varies as $h^{\frac{1}{2}}$ and a turbulent diffusivity that varies as $h^{\frac{3}{2}}$, so that

$$u(y) = \frac{\overline{u}\overline{h}h^{\frac{1}{2}}}{\overline{h^{\frac{3}{2}}}}, \quad \kappa_2(y) = \frac{\overline{\kappa}_2\overline{h}h^{\frac{3}{2}}}{\overline{h^{\frac{3}{2}}}} \tag{3.3}$$

(Smith 1981, equation (6.5)), although the effects of using different power laws on some of the results have also been investigated by Daish (1985). Whichever turbulence parametrization is adopted, explicit asymptotic expressions for the moments of the concentration can be derived in terms of q and the solutions of certain ordinary differential equations, as shown by Smith (1981, 1982*b*).

As $t \to \infty$ the zeroth moment tends to the constant value $\overline{q}$, whilst the asymptotic centroid displacement X is given by

$$X = \overline{gq}/\overline{q}, \tag{3.4}$$

the function $g(y)$ satisfying

$$\frac{\mathrm{d}}{\mathrm{d}y}\left(h\kappa_2\frac{\mathrm{d}g}{\mathrm{d}y}\right) = h(\overline{u}-u), \tag{3.5a}$$

with

$$h\kappa_2\frac{\mathrm{d}g}{\mathrm{d}y} = 0 \quad \text{on } y = 0, B, \tag{3.5b}$$

and

$$\overline{g} = 0 \tag{3.5c}$$

(Smith 1981). g is, in fact, simply the shape function of §2.

The form of the second moment can also be made more precise. Smith (1982*b*) finds that

$$\frac{c^{(2)}}{c^{(0)}} \sim 2Dt + 2g^{(2)}(y) + \frac{2\overline{g^{(2)}q}}{\overline{q}} - 2\overline{g^2}, \tag{3.6}$$

where

$$D = \overline{(u-\overline{u})g} \tag{3.7}$$

(cf. (2.7)) and $g^{(2)}$ satisfies

$$\frac{\mathrm{d}}{\mathrm{d}y}\left(h\kappa_2\frac{\mathrm{d}g^{(2)}}{\mathrm{d}y}\right) = h\{\overline{(u-\bar{u})g}-(u-\bar{u})\,g\}, \tag{3.8a}$$

with

$$h\kappa_2\frac{\mathrm{d}g^{(2)}}{\mathrm{d}y} = 0 \quad \text{on } y = 0, B, \tag{3.8b}$$

and

$$\overline{g^{(2)}} = 0. \tag{3.8c}$$

This means that the asymptotic variance of the cloud in the moving frame, Σ^2, is given by

$$\Sigma^2 \sim 2Dt - 2\overline{g^2} + \frac{2\overline{g^{(2)}q}}{\bar{q}} - \left(\frac{\overline{gq}}{\bar{q}}\right)^2. \tag{3.9}$$

4. A closer look at the variance, and how to influence it

Rewriting (3.9) in the form

$$\Sigma^2 \sim 2Dt + V, \tag{4.1}$$

so that V is given by

$$V = -2\overline{g^2} + \frac{2\overline{g^{(2)}q}}{\bar{q}} - \left(\frac{\overline{gq}}{\bar{q}}\right)^2, \tag{4.2}$$

we see that Σ^2 falls into two distinct parts. Each arises from an interaction between the shear and transverse diffusion, but reflects a different aspect of the dispersion process. Far downstream, concentrations vary little in a cross-section, and the longitudinal stretching effect of the shear and the transverse mixing are essentially in balance, acting together to increase Σ^2 steadily with time. We can therefore think of the first, time-dependent part as the contribution of the asymptotic regime itself to the variance, and, as we have already seen, it is independent of the initial concentration distribution. In contrast, the second part is time-independent, embodying the overall effect of the early stages of the dispersion on the variance, when large variations in the concentration exist across the channel rather than some equilibrium state. We shall call this second contribution the 'discharge variance'.

Figure 2 shows the general form of the variance as time evolves. The two elements of the variance can clearly be seen: the eventual linear growth rate after a time of order $B^2/\bar{\kappa}_2$ has elapsed (corresponding to a distance downstream of, typically, 100 channel breadths), but with the precise asymptote depending on the initial conditions through the discharge variance V.

Equations (3.9), (4.1) and (4.2) are all defined relative to the moving frame. For a fixed observer at position x downstream, say at the site of a water intake, it is natural to take $t = t_a \approx x/\bar{u}$, the time of arrival based on $\bar{u}$, in these expressions. However, it is then necessary to adjust the discharge variance by an amount $2DX/\bar{u}$, because the centroid displacement makes the cloud appear to arrive a time $X/\bar{u}$ earlier than expected. Thus we write the observed asymptotic variance Σ_0^2 in the form

$$\Sigma_0^2 \sim 2Dt_a + V_0, \tag{4.3}$$

where the 'adjusted discharge variance' V_0 (abbreviated to a.d.v.) is given by

$$V_0 = V - 2DX/\bar{u}. \tag{4.4}$$

(Note that this is the negative of the 'adjusted deficit variance' employed by Smith (1981).)

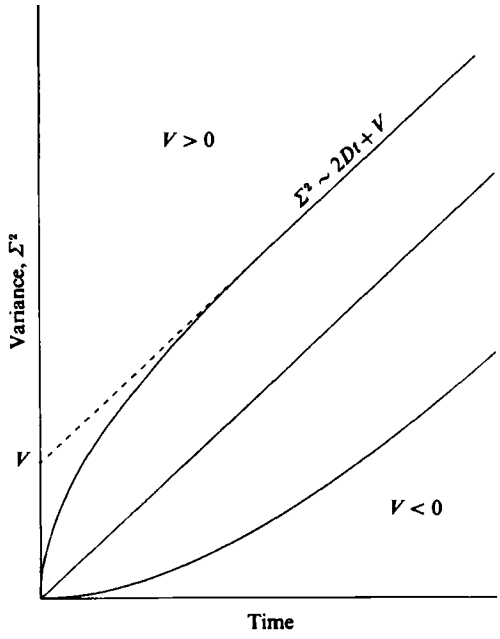

FIGURE 2. Schematic diagram of the growth of the variance of a contaminant cloud with time, in a frame moving with the bulk velocity $\bar{u}$.

The dichotomy in the contributions to (4.1) or (4.3) means that we can influence the variance, and therefore asymptotic concentration levels, in two different ways. First, the dispersion-coefficient term can be made larger by simply relocating the discharge further upstream, so that the time taken to arrive at a particular observation point is increased. Secondly, and more usefully, we can try to choose the initial distribution of contaminant, as characterized by q, to exploit the channel's non-uniformities as fully as possible, and so make V_0 as large as possible. It is this aspect of the optimization of Σ_0^2 that we shall be concerned with in the rest of this paper.

To see how this might be achieved, consider the topography of a typical natural channel such as that in figure 1. It has a zone of slow-moving shallow water near one or both of its banks, and a region of relatively fast-flowing and deep water around the middle. These two zones have quite different mixing characteristics: the shallow water has a lot of shear and little transverse mixing, whilst the deep water has only a small amount of shear together with rapid mixing across the flow. The shallow water has the additional advantage that it is slow-moving, so that there is the greatest possible time for the shear to act before the cloud reaches an observer. These remarks suggest that a discharge should be weighted towards the shallow part of a channel if greatest advantage is to be taken of these features in the early stages of the mixing.

5. Single-point discharge

In this section we briefly consider making the entire release at one point (as Smith (1981) did) and the effect of varying the position of that point, before asking whether there is any advantage in splitting this source up into a multipoint discharge in §6.

A single point source at $y = y_s$ can be represented by means of a Dirac delta function, taking

$$q(y) = \frac{\bar{q}A}{h}\delta(y-y_s). \tag{5.1}$$

The resulting expressions for the centroid displacement and the adjusted discharge variance are simple in form and only involve the auxiliary functions g and $g^{(2)}$ at the discharge point. The centroid displacement for such a discharge profile varies with y_s as the shape function g, i.e.

$$X = g(y_s), \tag{5.2}$$

and the a.d.v. is easily seen to be

$$V_0 = -2\overline{g^2} + l(y_s), \tag{5.3}$$

where

$$l(y) = 2g^{(2)}(y) - 2\frac{\overline{ug}}{\bar{u}}g(y) - \{g(y)\}^2. \tag{5.4}$$

From the considerations of §4, we would expect l – and therefore V_0 – to have a maximum when the discharge is located in shallow water, especially since the point release that we are considering represents the most extreme weighting of q possible. Such a region of shallow water is invariably provided by the channel near to one or both of its banks. Moving a point source away from this favourable location would enable the cloud to mix into the deeper central parts more rapidly, giving less of it a long time to be sheared out. Thus, provided the channel bed slopes sufficiently gently there, i.e. provided there is enough shallow water accessible to the cloud as it starts to disperse, one of the banks should afford a maximum in V_0. Conversely, a bank where the channel bed slopes sufficiently steeply will provide a bad choice of site, as moving a discharge away from such a bank will allow the cloud to mix into the advantageous shallow regions sooner, yielding a local minimum in V_0. This is also true of the deep parts of the channel interior, where we might expect a global minimum in the a.d.v.

Various examples of channels illustrating these and other general trends are shown in figure 3. They are all intended to represent a more 'normal' type of channel, with a variety of possible forms. The a.d.v. is shown as a function of y_s for each profile, and it is clear that the bank with the most shallow water accessible to it is the best site to choose. Figures 3(*a*, *d*) illustrate two of the simplest depth profiles commonly employed, namely with a symmetric triangular and trapezoidal cross-section respectively. They exhibit the characteristic minimum in V_0 for a release in the deep parts of the channel, rising to a maximum at the banks. Figures 3(*a*–*c*) show how the more gently sloping side is favoured in a simple triangular channel: as the asymmetry of the depth profile increases, so does the disparity in the a.d.v. at the two sides. When there are two shallow sides, the shallower is the better of the two, and the central regions of the channel become relatively unimportant, as illustrated in figures 3(*e*–*g*), whilst figure 3(*h*) shows that a wider stretch with the same slope will win.

Each graph of $V_0(y_s)$ in figure 3 has been normalized with $\overline{g^2}$. This quantity is an intrinsic property of any particular channel, as well as a natural scale for V_0, since the a.d.v. takes the value $-2\overline{g^2}$ when the discharge is uniform ($q \equiv \bar{q}$). This means that $\overline{g^2}/\overline{ug}$ can be interpreted as a time for cross-sectional mixing, t_m, so that the time t_c when the dispersion coefficient and a.d.v. contributions become comparable in size is given by

$$t_c = \frac{1}{2}\frac{V_0}{\overline{g^2}}t_m, \tag{5.5}$$

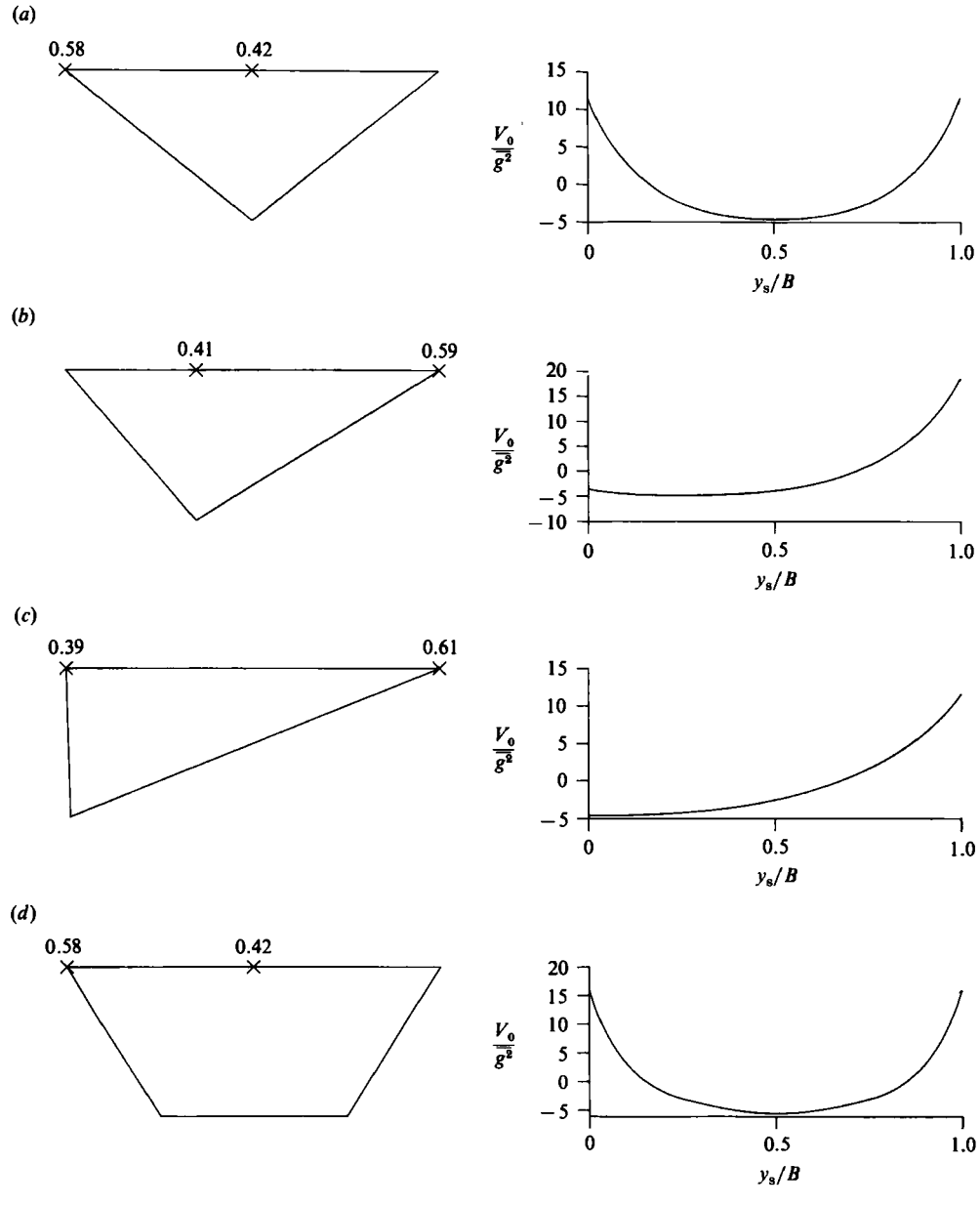

FIGURE 3(*a–d*). For description see facing page.

i.e. a certain number of 'mixing times'. So the fact that the numbers on the V_0 axes in figure 3 are frequently large shows that the influence of the a.d.v. extends over a considerable distance downstream after mixing across the flow has occurred. Furthermore, the influence itself is a significant one, as the a.d.v. is usually positive at the banks, so that the total variance is increased beyond its value given simply by the dispersion coefficient, and usually significantly so over its value for a uniform discharge.

Figure 4 shows what can happen if there is an alternative region of shallow water

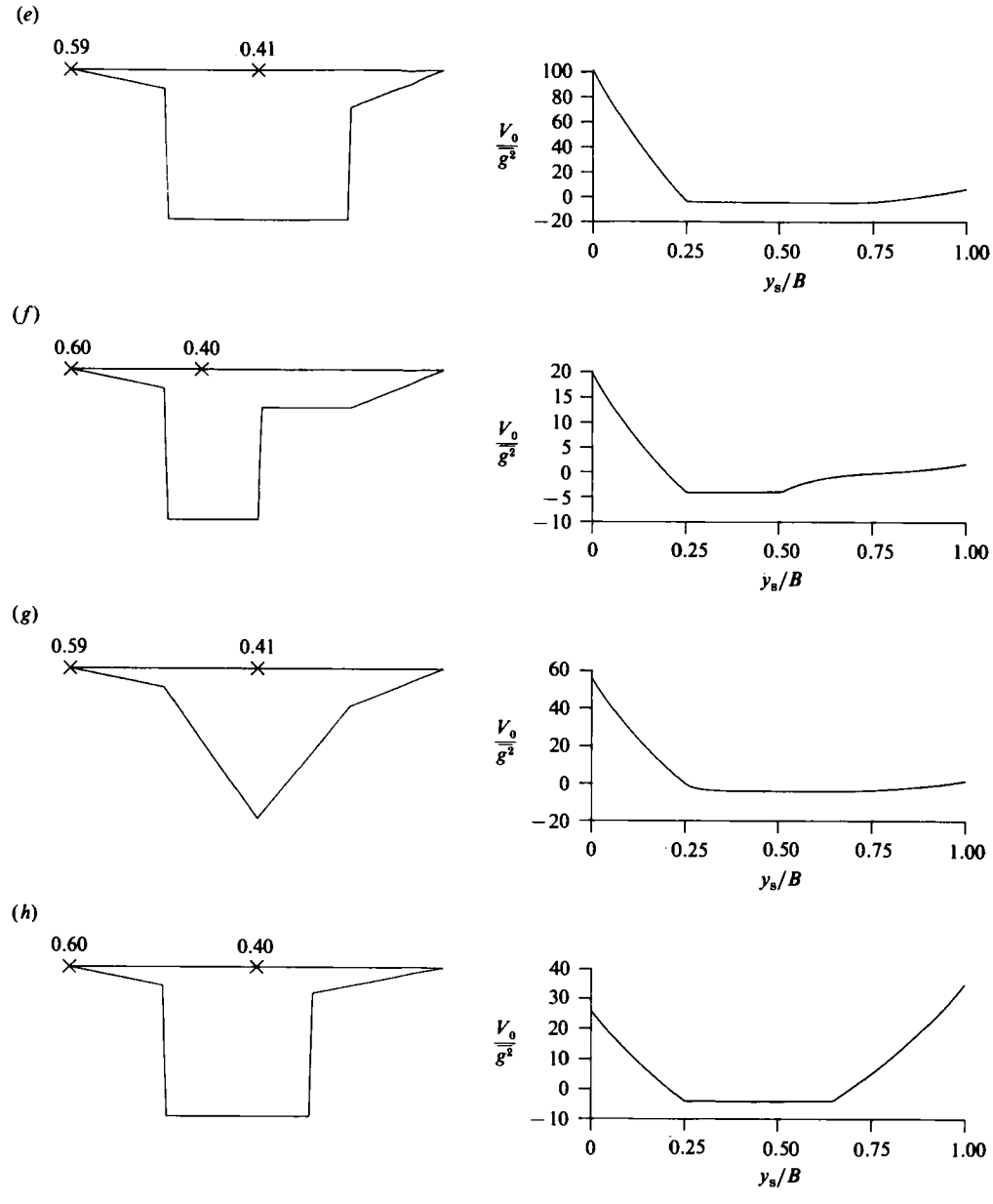

FIGURE 3. Adjusted discharge variance for some normal depth profiles. The crosses indicate optimal positions for two sources, and the numbers above their weightings.

present in the channel, in this case a rise at its centre. As it gets progressively higher, the a.d.v. becomes more and more peaked for a release at the centre of the channel. The shallowest bank ($y = B$) is initially the optimal site, as in figure 4(*a*), but this is eventually replaced by the centre as the rise grows to within $\frac{1}{4}H$ of the surface. Note that the banks are local maxima in figure 4(*c*), even though neither corresponds to the overall maximum for V_0; this shows the condition given by Smith (1981) for a bank to be a local extremum of the a.d.v. (sufficiently shallow slope to the channel bed) does not always give the best choice of site.

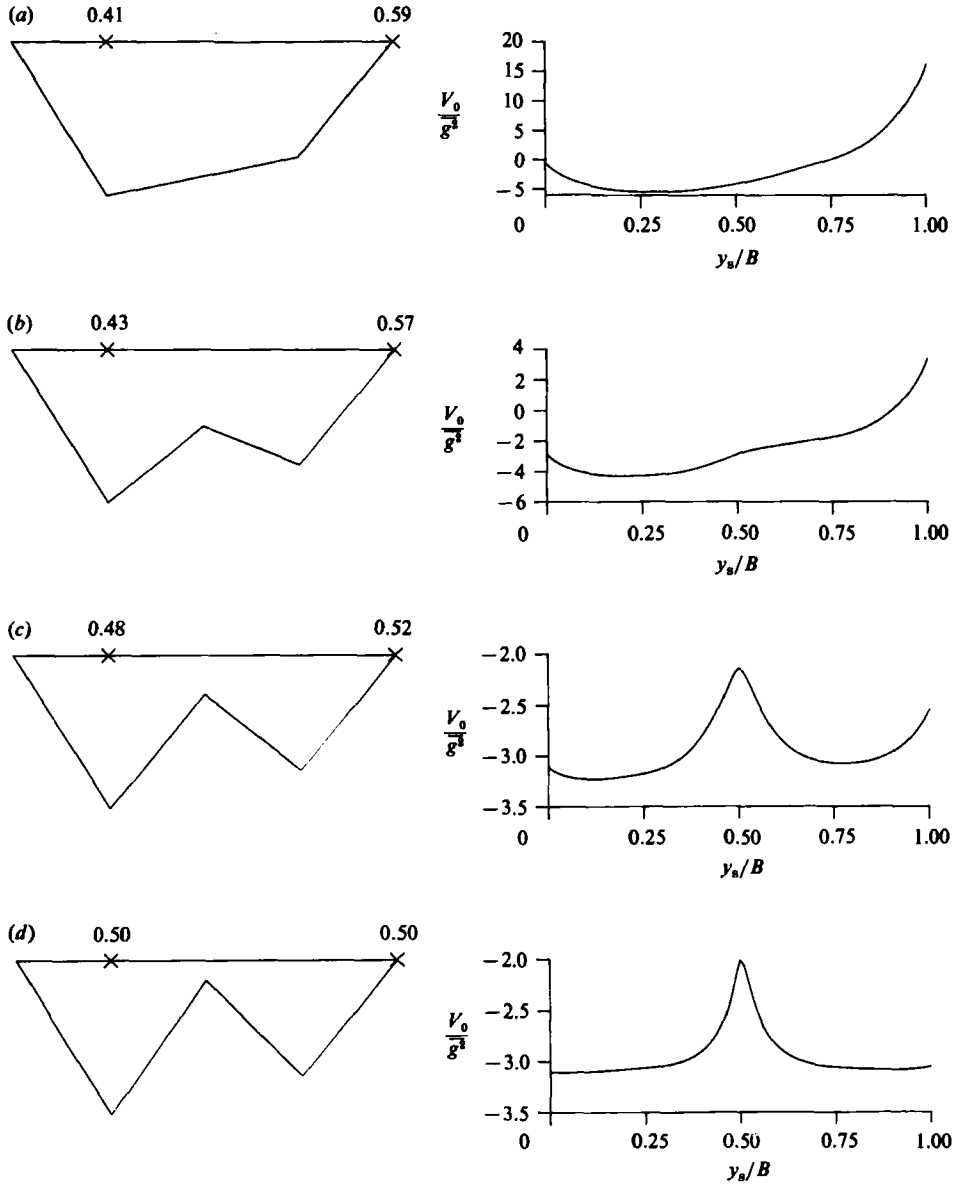

FIGURE 4. Adjusted discharge variance for a sequence of channels with an increasingly prominent rise at $y = \frac{1}{2}B$. Depth of channel at this point is (*a*) $\frac{7}{8}H$, (*b*) $\frac{1}{2}H$, (*c*) $\frac{1}{4}H$ and (*d*) $\frac{1}{8}H$.

In all cases, it should be noted that there is a price to pay when the discharge is localized in the shallow water, namely very high concentrations near to the release. The shallower the water, the higher these initial concentrations will be, since it is clear that $c \propto h^{-1}$ in the vicinity of the discharge.

6. Multipoint discharge

The results of §5 amply demonstrate that a prudent choice of q can have a significant effect on the state of a contaminant cloud in the asymptotic regime. We

now consider whether subdividing the single-point release into a number of distinct parts can significantly further increase the variance, and find that it can do in a surprisingly simple way.

Generalizing to a combination of n point discharges located at $y_1, y_2, \ldots, y_n$ with non-negative weightings $\alpha_1, \alpha_2, \ldots, \alpha_n$, the profile q becomes

$$q(y) = A\bar{q} \sum_{j=1}^{n} \frac{\alpha_j}{h} \delta(y - y_j), \tag{6.1}$$

where

$$\sum_{j=1}^{n} \alpha_j = 1, \tag{6.2}$$

so that (6.1) corresponds to the same total amount of contaminant as (5.1).

The centroid displacement now becomes a weighted average of values of g:

$$X = \sum_{j=1}^{n} \alpha_j g(y_j), \tag{6.3}$$

whilst the a.d.v. can be written

$$V_0 = -2\overline{g^2} + L, \tag{6.4}$$

$L(y_1, y_2, \ldots, y_n, \alpha_1, \alpha_2, \ldots, \alpha_n)$ being defined by

$$L = \sum_{j=1}^{n} \alpha_j E_j - \left\{ \sum_{j=1}^{n} \alpha_j g_j \right\}^2, \tag{6.5}$$

where

$$g_j = g(y_j), \quad l_j = l(y_j) \tag{6.6a}$$

and

$$E_j = g_j^2 + l_j \tag{6.6b}$$

with l as in (5.3).

We must therefore maximize L subject to (6.2); introducing the Lagrange multiplier λ, this means maximizing

$$L - \lambda \left\{ \sum_{j=1}^{n} \alpha_j - 1 \right\} \tag{6.7a}$$

subject to

$$\sum_{j=1}^{n} \alpha_j = 1 \tag{6.7b}$$

with

$$\alpha_j \geqslant 0 \quad (j = 1, 2, \ldots, n) \tag{6.7c}$$

and

$$0 \leqslant y_j \leqslant B \quad (j = 1, 2, \ldots, n). \tag{6.7d}$$

We have already seen (when $n = 1$) that the optimal solution can lie on the boundary of the domain occupied by our set of variables: one release site is usually at $y = 0$ or B. We must therefore exercise care in using differentiation techniques to find the solution of (6.7).

If there are more than two distinct sources in this solution, then only two can have $y = 0$ or B; so suppose two of the $\{y_j\}$ are fixed for the moment – say y_1 and y_2 – but that the other sites and all the weightings are undetermined, with none of the $\{\alpha_j\}$ equal to zero or one. Then, upon varying the remaining variables, we must satisfy the equations

$$\alpha_j(E_j' - \mu g_j') = 0 \quad (j = 3, \ldots, n) \tag{6.8a}$$

and

$$E_j - (\lambda + \mu g_j) = 0 \quad (j = 1, \ldots, n), \tag{6.8b}$$

where

$$\mu = 2 \sum_{k=1}^{n} \alpha_k g_k \tag{6.8c}$$

and $$g'_j = g'(y_j), \quad E'_j = E'(y_j), \tag{6.8d}$$

subject to the same constraints appearing in (6.7).

Then, without solving (6.8*a*, *b*), the extremal value of L can be written down: using the definition of L, together with (6.7) and (6.8), we find

$$L = \tfrac{1}{4}\mu^2 + \lambda. \tag{6.9}$$

Moreover, λ and μ can be eliminated in favour of say y_1 and y_2 (provided $\alpha_1, \alpha_2 \neq 0$ or 1), since

$$\lambda = \frac{E_2 g_1 - E_1 g_2}{g_1 - g_2} \tag{6.10}$$

and

$$\mu = \frac{E_1 - E_2}{g_1 - g_2}. \tag{6.11}$$

Thus the optimal value of L can be expressed entirely in terms of y_1 and y_2. The other equations (namely (6.8*a*), and (6.8*b*) for $j = 3, \ldots, n$) can be satisfied if we take the remaining $\{y_j\}$ to be either y_1 or y_2, choosing whichever is not at a boundary – we shall see *a posteriori* that this is possible. We therefore conclude that we need only two sources to optimize V_0, at least one of which must be in the interior of the channel. Henceforth we restrict attention to the two-source problem.

In looking for the optimal positions and weightings of these two sources, it should be noted that if we expand L about the weightings (α_1^*, α_2^*) satisfying (6.8*b*), with y_1 and y_2 fixed, L is non-decreasing with respect to variations in α_1 and α_2. The optimal weightings are therefore given by

$$\alpha_1^* = \frac{1}{2}\left\{1 + \frac{l_1 - l_2}{(g_1 - g_2)^2}\right\}, \quad \alpha_2^* = \frac{1}{2}\left\{1 - \frac{l_1 - l_2}{(g_1 - g_2)^2}\right\}. \tag{6.12a, b}$$

Bearing in mind that a single site should usually be at one of the banks, we expect one part of a split discharge to remain at that good bank. Numerical evaluations of V_0 were carried out for a wide range of piecewise-linear depth profiles, allowing V_0 to be calculated exactly. In each case once g and l had been found, α_1 and α_2 were set to their optimal values (6.12) for each (y_1, y_2), and all points in the allowed range searched through to find the discharge sites with non-negative weightings giving the maximum value of V_0. These calculations revealed that one part of the discharge should indeed be made at the best bank for a single point source, whilst the other part is best released in the channel interior, near to where the flow is greatest. These findings justify the remarks made after (6.10) and (6.11).

So, choosing $y_1 = 0$ (or B), y_2 can be found from (6.8*a*, *b*):

$$\frac{E'_2}{g'_2} = \frac{E_1 - E_2}{g_1 - g_2}. \tag{6.13}$$

Equations (6.9)–(6.11) will then give L, and hence V_0. y_1 and y_2 must, of course, satisfy the criterion

$$|l_1 - l_2| \leqslant (g_1 - g_2)^2 \tag{6.14}$$

to ensure that the weightings lie in the range 0–1.

7. Example: triangular channel

In this section we give a simple example, for which all the above results can be obtained analytically, in order to illustrate these ideas. Consider a channel whose depth-profile is an isosceles triangle (see figure 3*a*); we may then make direct comparisons with Smith (1981, §7). For this symmetric depth profile we take the channel to have breadth $2B$ (rather than B as we have done in previous sections) and to occupy $0 \leqslant y \leqslant 2B$; its symmetry also means that we need only consider one half, say $0 \leqslant y \leqslant B$.

Integrating (3.5*a*) and (3.8*a*) for g and $g^{(2)}$, using the $h^{\frac{1}{2}}$ and $h^{\frac{3}{2}}$ power laws for u and κ_2 respectively, we find after some algebra that g and l are given by

$$g = \left(\frac{14\overline{g^2}}{31}\right)^{\frac{1}{2}}(-14+30\,Y^{\frac{1}{2}}-15\,Y), \tag{7.1a}$$

$$l = \frac{\overline{g^2}}{31}\{419-100(24\,Y-28\,Y^{\frac{3}{2}}+9\,Y^2)\}, \tag{7.1b}$$

and therefore

$$E = \frac{\overline{g^2}}{31}(3163-11760\,Y^{\frac{1}{2}}+16080\,Y-9800\,Y^{\frac{3}{2}}+2250\,Y^2) \tag{7.1c}$$

where $Y = y/B$ (see Smith 1981, equations (7.7), (7.10) and (7.11)). (Writing these expressions in terms of $\overline{g^2}$ renders them independent of the precise choice of coefficient in the power laws for u and κ_2; in fact, $\overline{g^2}/31 = (2/77175)\,B^4\overline{u}^2/\overline{\kappa}_2^2$.)

The best site for a single discharge in this half of the channel is at $y = 0$, so, taking $y_1 = 0$, (6.13) for possible $Y_2 = y_2/B$ becomes

$$Y_2^{\frac{1}{2}}(Y_2^{\frac{1}{2}}-1)(225\,Y_2-940\,Y_2^{\frac{1}{2}}+1020) = 0. \tag{7.2}$$

The last factor on the left-hand side has complex roots, so (reverting to y_1 and y_2) the real roots of (7.2) are $y_2 = 0$ and $y_2 = B$.

The first solution simply corresponds to combining both parts at $y = 0$, as considered by Smith (1981); for this choice of y_2 the value of the a.d.v. is

$$V_0 = 357\frac{\overline{g^2}}{31}. \tag{7.3}$$

However, if we select $y_2 = B$, (6.9) and (7.1) yield

$$V_0 = \frac{115207}{126}\frac{\overline{g^2}}{31} \approx 914.34\frac{\overline{g^2}}{31}. \tag{7.4}$$

This is an increase in the size of the contribution of the a.d.v. by a factor of over two.

Finally, (6.12) tells us that the weightings should be

$$\alpha_1 = \frac{73}{126}, \quad \alpha_2 = \frac{53}{126} \tag{7.5}$$

so that the discharge is more heavily weighted in favour of the good bank, as anticipated.

Figure 5 shows a contour plot of $V_0(y_1, y_2, \alpha_1^*, \alpha_2^*)$ for this triangular channel. Because α_1 and α_2 have been set to their optimal values (6.12), they may be non-positive for certain choices of (y_1, y_2), so that only the area between the dotted line and the boundary is relevant. It is clear that there is a rapid decrease in V_0 as y_1 is moved

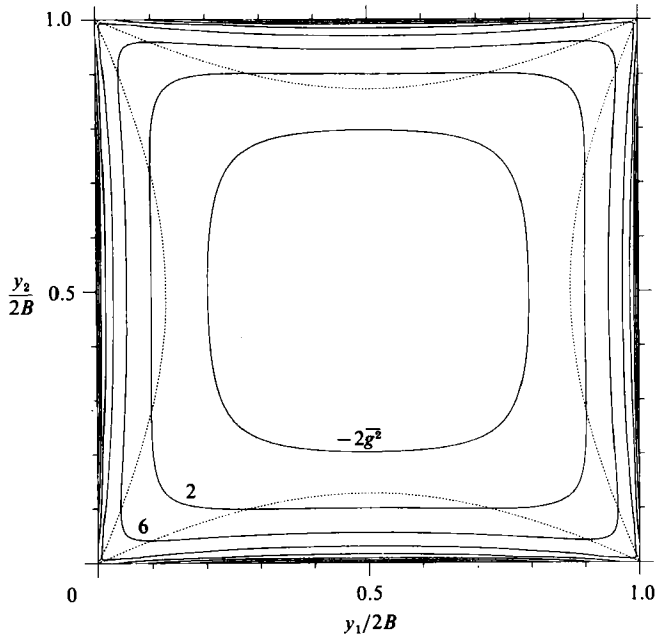

FIGURE 5. Contour plot of the adjusted discharge variance for a symmetric triangular channel, as a function of the discharge positions. Only the region between the dotted line and the boundary is physically relevant.

away from the bank, whilst there is again a decrease in V_0, though a much gentler one, as y_2 is moved away from the centreline.

If we now keep y_1 and y_2 fixed at their optimal positions and allow α_1 and α_2 to vary between 0 and 1 (subject to the constraint (6.2)), the a.d.v. varies with α_1, say, according to

$$V_0 = (3150\alpha_1^2 - 3650\alpha_1 + 143)\frac{\overline{g^2}}{31}. \tag{7.6}$$

This is plotted in figure 6, and shows a significant reduction in V_0 when there is little of one or other source, but a peak at our optimal choice of a split source.

The conclusions of this section have all been based on the power-law parametrization (3.3) of the turbulent mean velocity and transverse diffusivity profiles. It can be shown (see Daish 1985) that the same conclusions arise for the triangular channel when we allow different powers of h in the formulation. Specifically, if u varies as h^r and κ_2 as h^{2-r} (which follows from the assumption that κ_2 scales with depth in the same way as the vertical eddy viscosity), then, provided $0 < r < 4$ (which includes all possible cases of interest):

(i) either bank is the best choice for a single discharge;

(ii) a split discharge should be made with one part (more heavily weighted) at a bank, and the remainder in the middle of the channel;

(iii) the a.d.v. for two optimally sited sources is always larger than for a single release at a bank.

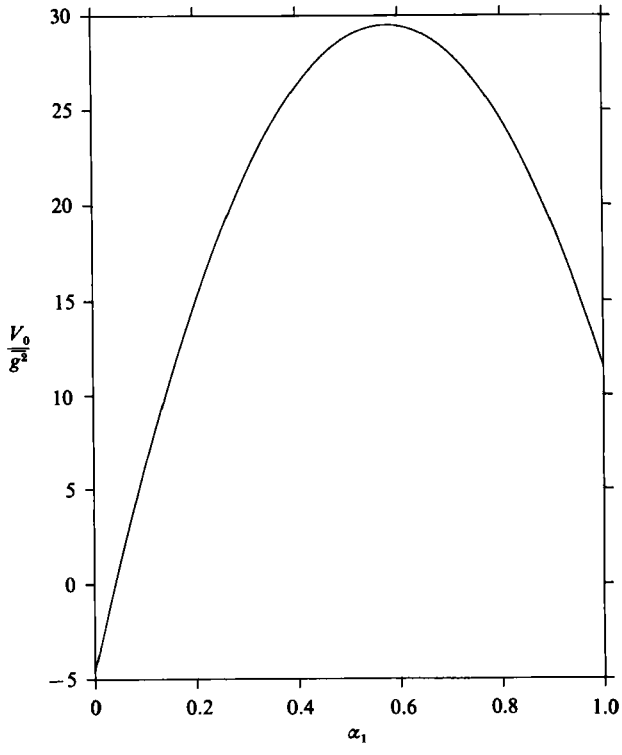

FIGURE 6. Adjusted discharge variance for a symmetric triangular channel as a function of the weighting of the source at the bank when the two sources are optimally located.

8. Mean-concentration profiles

Having found the optimal location and weightings for the discharges, what does this mean in terms of concentrations? The fact that the second part of the discharge should go where the flow is fast means that the two parts will initially separate quite rapidly, hence automatically increasing the variance. This disparity in their behaviour suggests that there may not be any significant interaction between them (a feature potentially masked by a consideration of the variance alone), and that it will simply appear to an observer that two disjoint clouds are passing by.

We may obtain an idea of how the cross-sectionally averaged concentration evolves by considering a simple one-term Gaussian approximation for each part. In a frame moving with the bulk velocity $\bar{u}$, a first approximation to the mean concentration $\bar{c}$ of a contaminant cloud due to a point discharge made at $y = y_s$ is given by

$$\bar{c}(x,t;y_s) = \frac{\bar{q}}{(2\pi)^{\frac{1}{2}} A\Sigma} \exp\left\{-\frac{(x-X)^2}{2\Sigma^2}\right\}, \tag{8.1}$$

where Σ^2 is the variance of the cloud in the moving frame, as detailed in (3.9). We take the two parts of the release to evolve independently, and the concentration due to both to be the linear superposition of the two Gaussian profiles that emerge far downstream. We also assume that the asymptotic separation of the two centroids has been attained; this is consistent with the use of a Gaussian profile for $\bar{c}$. Insofar as we eventually obtain two blobs of contaminant separated by a fixed distance along the flow, this situation has been discussed by Chatwin (1972, §3).

We saw earlier that the mean concentration will evolve as per a one-dimensional diffusion equation once the deviations from the mean are small. Smith (1979) calculated an e-folding time t_e for the decay of these deviations, which may be written as

$$t_e = 7.9(\overline{g^2})^{\frac{1}{2}}/\overline{u} \tag{8.2}$$

(Smith 1981, equation (7.13)). (t_e will be of the same order of magnitude as t_m, the timescale for mixing across the flow in §5.) This means that, after n e-folding times have elapsed, the total variance due to a point source at $y = y_s$, $\Sigma^2_{1,n}$, will be given by

$$\Sigma^2_{1,n} = (3.08n + 7.90)\,\overline{g^2} \quad \text{when } y_s = 0, \tag{8.3a}$$

and

$$\Sigma^2_{1,n} = (3.08n - 4.36)\,\overline{g^2} \quad \text{when } y_s = B. \tag{8.3b}$$

So, if $\bar{c}_{1,n}(x; y_s)$ denotes the mean concentration at $t = nt_e$ due to one source, the mean-concentration field due to the optimal split source will be

$$\bar{c} = \tfrac{73}{136}\bar{c}_{1,n}(x; 0) + \tfrac{63}{136}\bar{c}_{1,n}(x; B), \tag{8.4}$$

i.e. a linear combination of the profiles for the best and worst choice of site for a single point source.

The concentration profile (8.4) for the split source together with that for a single point discharge at the best and worst sites are plotted in figure 7 at (*a*) 3 and (*b*) 6 e-folding times after release. At $t = 3t_e$ the split source has achieved a reduction in peak concentration over the single source at a bank, and both are significantly better than the single source at the middle of the channel. By $t = 6t_e$, the split source is forming itself into a single Gaussian-like profile whose peak concentration is only $\frac{2}{3}$ of that for the best single source (which is a greater relative reduction than between the best and worst single-source sites). If we were to follow the evolution of these profiles still further, we would eventually be in the true 'Taylor regime', where the $2Dt$ part of Σ^2_0 has become dominant and V_0 may be neglected altogether. Note, however, that the dispersion coefficient contribution to the variance is still significantly smaller than the a.d.v. at the later of the two times, so these reductions may genuinely be attributed to the choice of discharge conditions. (In fact, from (7.4) and (8.3), we see that over 9 e-folding times would have to elapse before the two contributions are equal in magnitude.)

9. The general depth profile: discussion and conclusions

The calculations of §7 were also made, numerically, for a wide variety of depth profiles, some of which were shown in figures 3 and 4. They concluded that, unless the channel topography was particularly unusual, the same procedure is applicable to a general depth profile. The bank which has the most shallow water accessible to it (i.e. the one where the channel bed slopes most gently) is the site to choose for the greater part of the discharge, whilst the other part of the release should be made near to the deepest part of the channel. The crosses on the channel depth profiles in figures 3 and 4 denote these optimal positions, and the numbers above refer to their respective weightings. Figure 4 also demonstrates the greater robustness of the double source to changes in the channel topography. In fact, the central peak would have to rise to within $H/100$ of the surface before both the optimal locations lie in the channel interior. This was found for many other examples for which neither bank offered the best site.

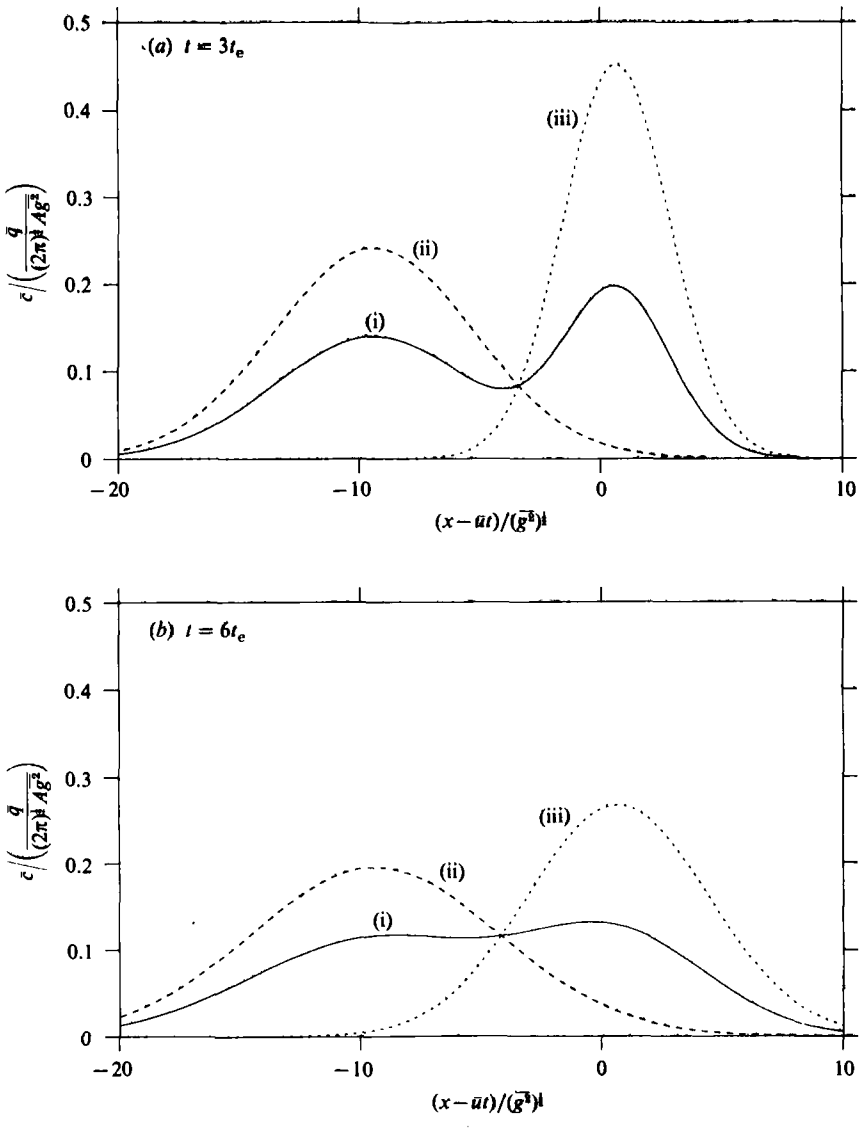

FIGURE 7. Mean-concentration profiles for a symmetric triangular channel at different times after release, in a frame moving with the bulk velocity $\bar{u}$. In each case, the profiles are those produced by (i) the optimal split source, (ii) a single source at a bank and (iii) a single source at the centre of the channel.

The numerical studies also showed that, in general, the a.d.v. is markedly improved when a single source is split into two appropriately placed and weighted parts, as we saw for the symmetric triangular channel. The increase was generally by a factor of 1.5 or more for all 'normal' depth profiles, so we would expect similar relative reductions in the peak concentrations to those in figure 7. Exceptions to this were channels for which a bank is not best, such as those with a rise in their interior; for these the cloud from a single source is able to disperse in two regions of shallow water instead of just one, so the a.d.v. produced by our procedure is comparable to this, and little advantage is gained by splitting the source.

The effect of this improvement in the a.d.v. by our method can be interpreted in two ways. Since it now takes longer for the dispersion-coefficient contribution to match that of the discharge conditions in magnitude (as D is the same whichever initial conditions we take), we can say that concentrations are reduced over a longer stretch downstream. Equation (5.5) shows that the region of influence increases in proportion to the increase in the a.d.v. Alternatively, we can say that they are further reduced over a certain part of the channel, compared to their values for a single point release.

How might these conclusions be modified for a longitudinally varying channel? Smith (1984) has calculated the variance of a contaminant cloud in such a non-uniform flow, and shows that it has the same general form as in the uniform case. However, the extra degrees of freedom render the corresponding optimal discharge analysis intractable. To some extent, the benefits of a split discharge are likely to be reduced by the secondary motions induced by any bends present, but it should still be the case that the same exploitation of the fast- and slow-moving parts of the flow will improve the dispersion and reduce peak concentrations in a general non-uniform channel.

We have seen that we can usually take two point sources to make the a.d.v. as significant as possible. The question then arises as to whether this is the best possible choice for q in (3.1); the answer to this must be 'yes' for the following reason. The number n of point sources in the distribution (6.1) was arbitrary, yet the solution turned out to be independent of how many there were. Any realistic type of release could necessarily only be made at a finite number of discrete points, as considered here, whilst some continuous distribution for q could be approximated by an arbitrarily large number of point sources, though just two would still yield the best a.d.v. We therefore conclude that our procedure will optimize the asymptotic shear dispersion of a sudden contaminant release for all but the most unusual uniform straight channels.

The author would like to acknowledge the financial support of the Science and Engineering Research Council.

REFERENCES

Aris, R. 1956 On the dispersion of a solute in a fluid flowing through a tube. *Proc. R. Soc. Lond.* A **235**, 67–77.

Chatwin, P. C. 1972 The cumulants of the distribution of concentration of a solute dispersing in solvent flowing through a tube. *J. Fluid Mech.* **51**, 63–67.

Daish, N. C. 1985 Shear dispersion in open channel flows. Ph.D. thesis, University of Cambridge.

Fischer, H. B., List, E. J., Koh, R. C. Y., Imberger, J. & Brooks, N. H. 1979 *Mixing in Inland and Coastal Waters.* Academic.

Smith, R. 1979 Calculation of shear dispersion coefficients. In *Mathematical Modelling of Turbulent Diffusion in the Environment* (ed. C. J. Harris), pp. 343–362. Academic.

Smith, R. 1981 The importance of discharge siting upon contaminant dispersion in narrow rivers and estuaries. *J. Fluid Mech.* **108**, 43–53.

Smith, R. 1982*a* Where to put a steady discharge in a river. *J. Fluid Mech.* **115**, 1–11.

Smith, R. 1982*b* Gaussian approximation for contaminant dispersion. *Q. J. Mech. Appl. Maths* **35**, 345–366.

Smith, R. 1984 Temporal moments at large distances downstream of contaminant releases in rivers. *J. Fluid Mech.* **140**, 153–174.

TAYLOR, G. I. 1953 Dispersion of soluble matter in solvent flowing slowly through a tube. *Proc. R. Soc. Lond.* A **219**, 186–203.

TAYLOR, G. I. 1954*a* The dispersion of matter in turbulent flow through a pipe. *Proc. R. Soc. Lond.* A **223**, 446–468.

TAYLOR, G. I. 1954*b* Conditions under which dispersion of a solute in a stream of solvent can be used to measure molecular diffusion. *Proc. R. Soc. Lond.* A **225**, 473–477.